MICROWAVE AND OPTICAL TECHNOLOGY LETTERS

Self-sustainable wireless sensor network for low-temperature application

Journal:	*Microwave and Optical Technology Letters*
Manuscript ID	MOP-21-0954.R1
Wiley - Manuscript type:	Research Article
Date Submitted by the Author:	10-Oct-2021
Complete List of Authors:	Cho, Young Seek; Wonkwang University Choi, Kyeongjun; Wonkwang University Kwon, Jaerock; University of Michigan-Dearborn
Keywords:	Energy harvester, low temperature, supercapacitor, wireless sensor network (WSN)

Note: The following files were submitted by the author for peer review, but cannot be converted to PDF. You must view these files (e.g. movies) online.

WileyNJD-v2.cls
NJDnatbib.sty
WileyNJD-AMA.bst
WSN_WPT.bib

John Wiley & Sons

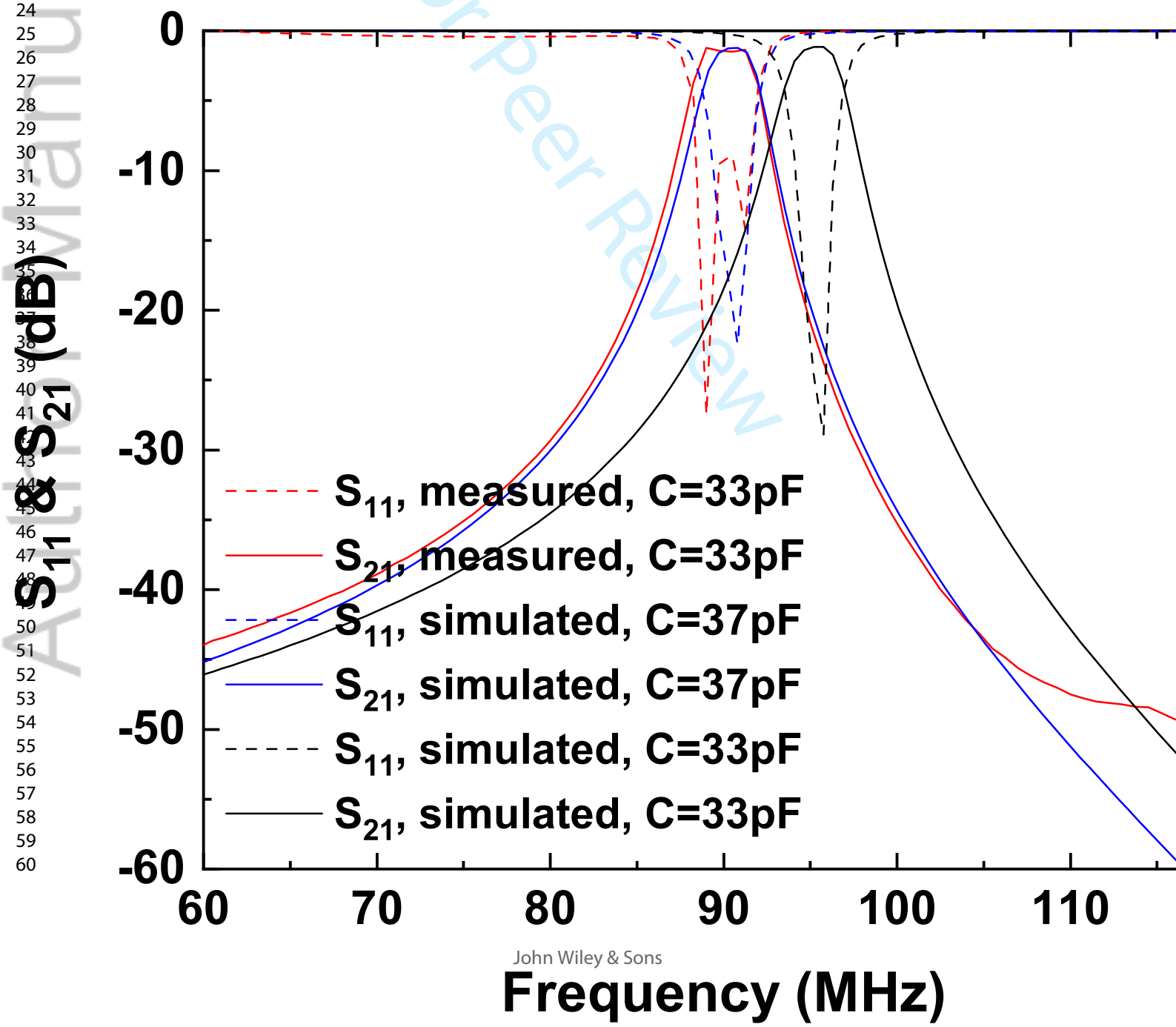

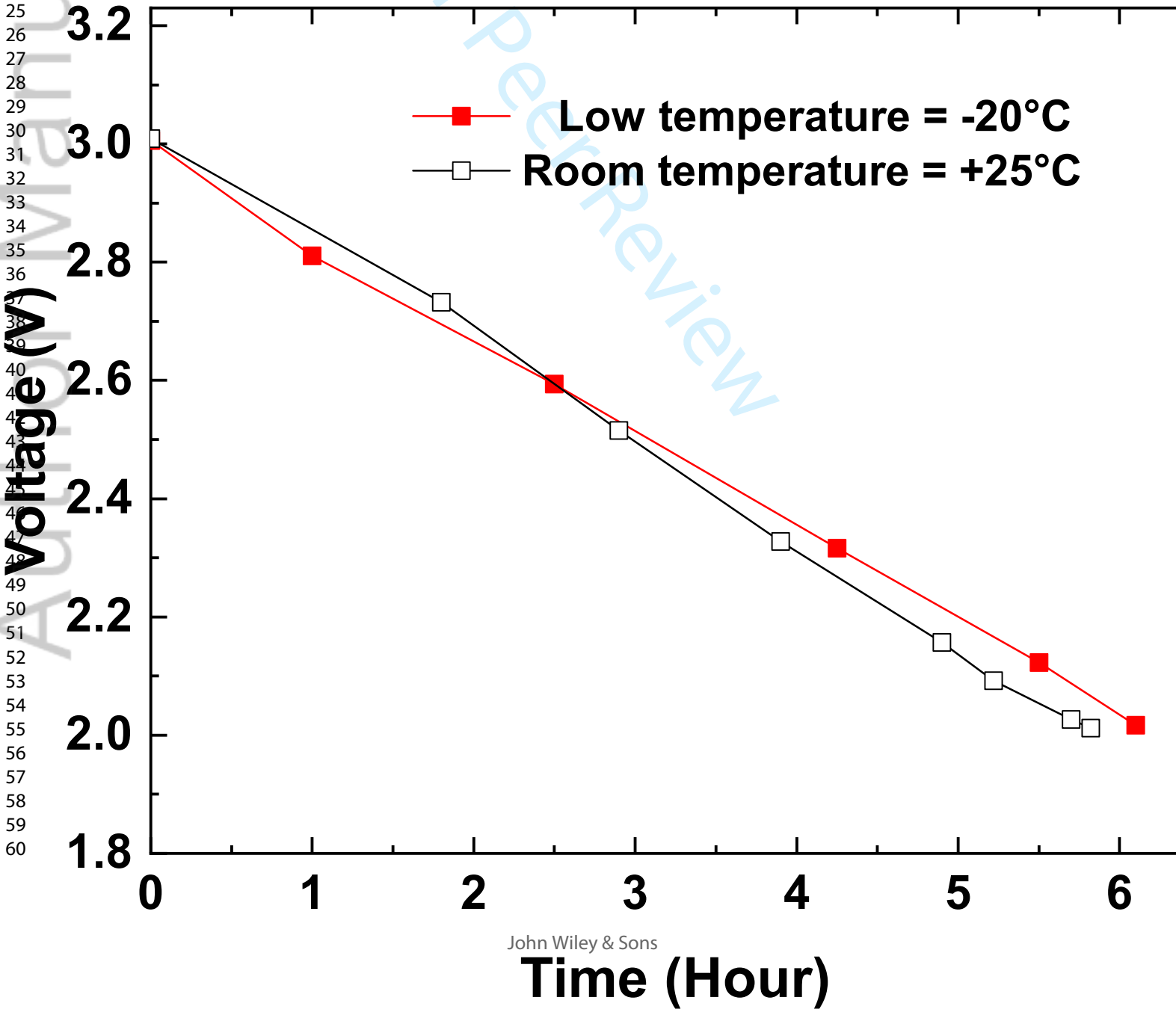

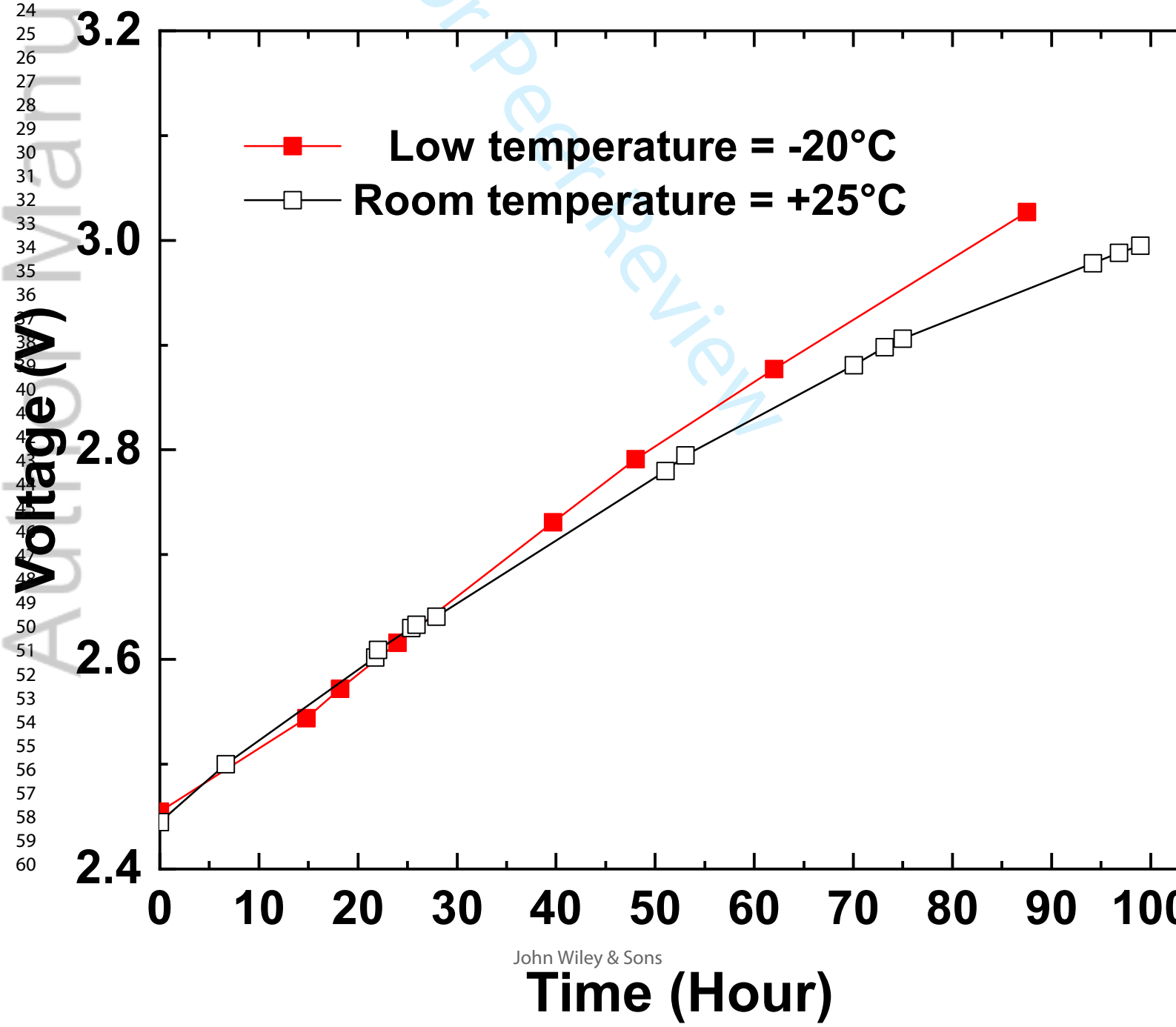

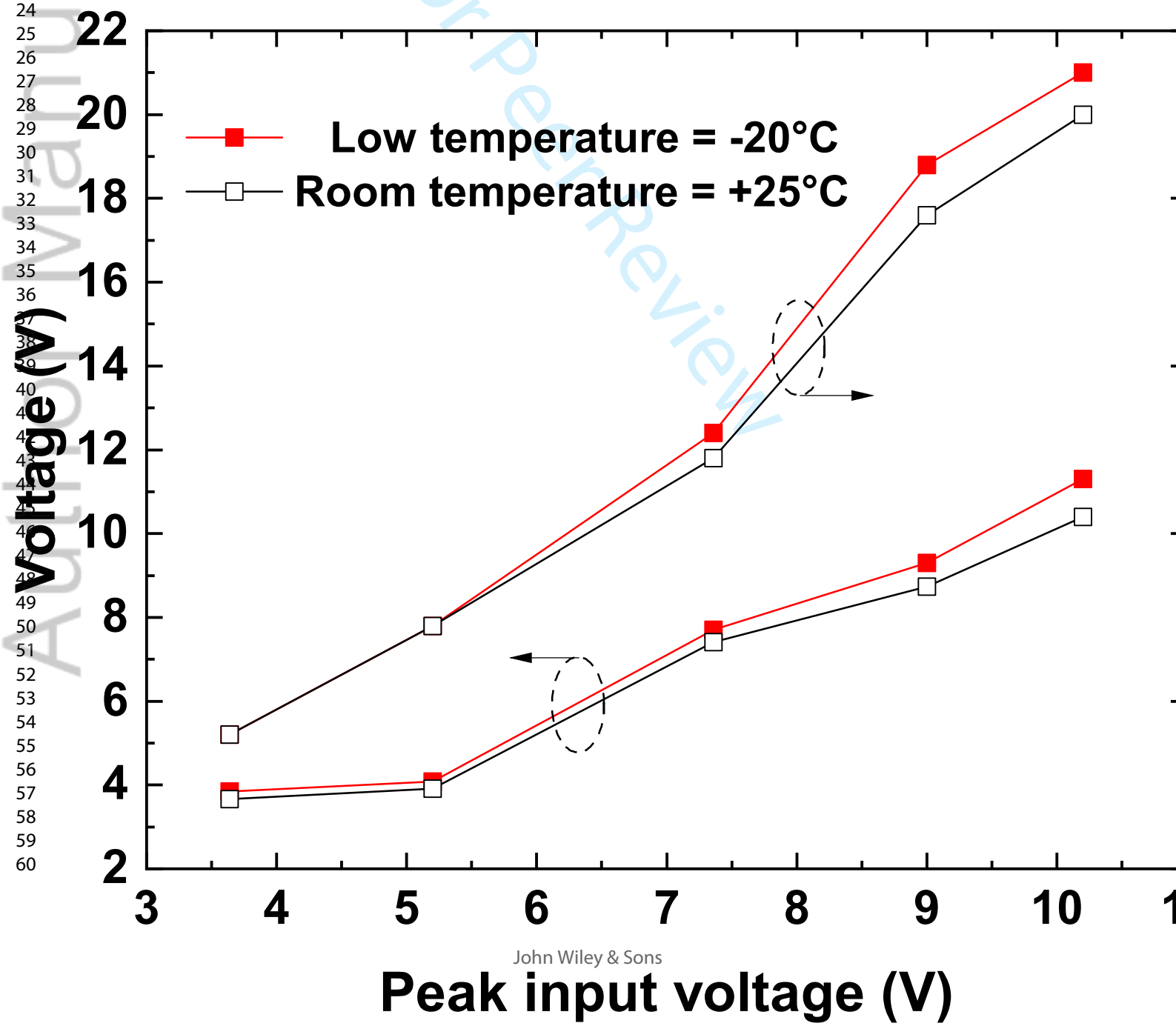

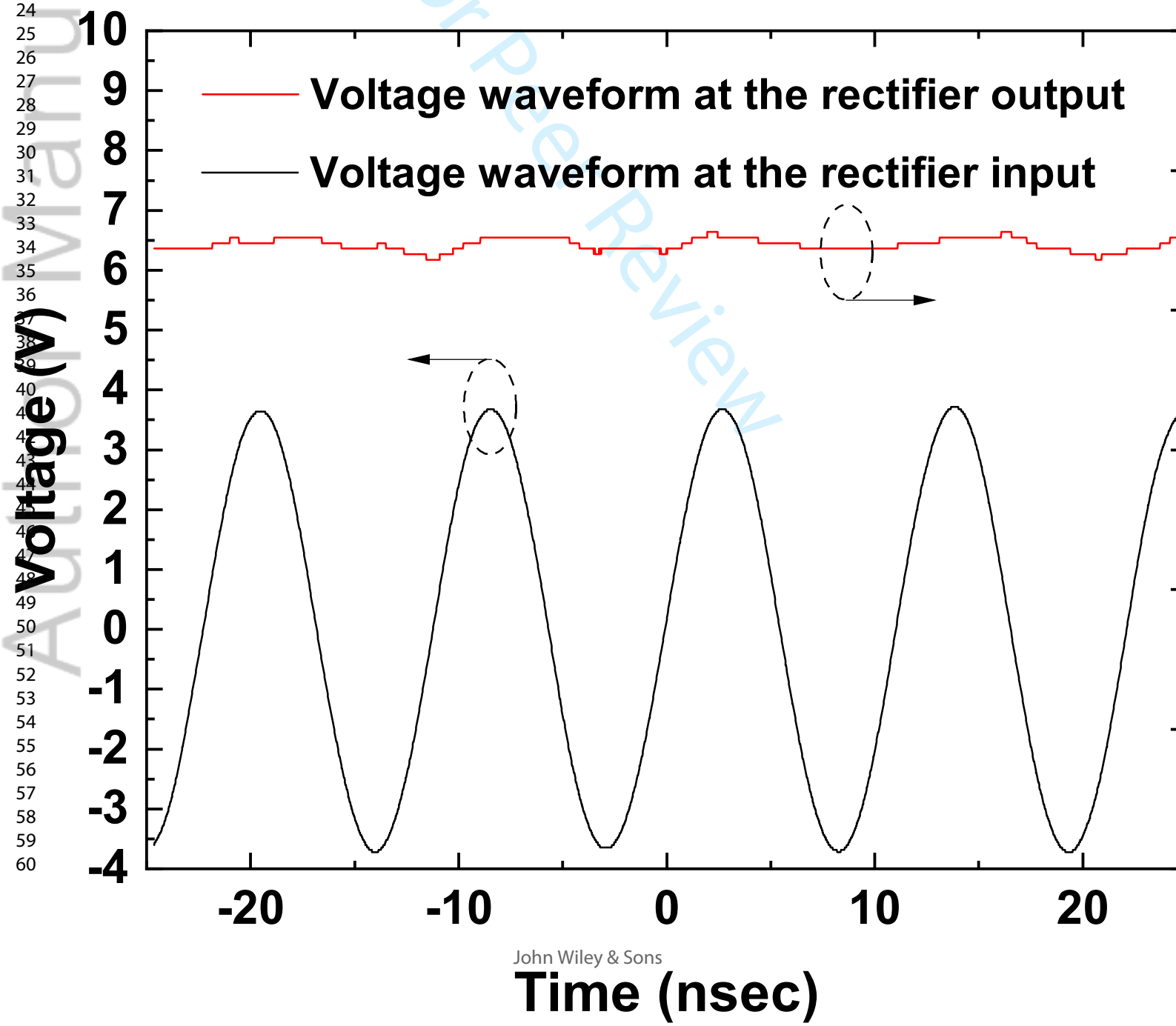

Received 29 July 2021; | Revised 6 June 2016; | Accepted 6 June 2016

DOI: xxx/xxxx

RESEARCH ARTICLE

Self-sustainable wireless sensor network for low-temperature application

Young Seek Cho*[1] | Kyungjoon Choi[2] | Jaerock Kwon[3]

[1]Department of Electronic Engineering, Wonkwang University, Jeollabuk-do, Republic of Korea
[2]Department of Information and Communication Engineering, Wonkwang University, Jeollabuk-do, Republic of Korea
[3]Department of Electrical and Computer Engineering, University of Michigan-Dearborn, Dearborn, MI, USA

Correspondence
*Young Seek Cho, Email: ycho@wku.ac.kr

Present Address
Department of Electronic Engineering, Wonkwang University, Iksan-si, Jeollabuk-do, 54538 Republic of Korea

Abstract

While environmental monitoring system is an exemplary application for wireless sensor network (WSN), its energy-constraint still remains unresolved issue and needs to be addressed. In this work, a self-sustainable WSN is proposed for low-temperature application. To resolve the energy-constraint issue, a wireless power transfer (WPT) technique, called conformal strongly coupled magnetic resonant (CSCMR) technique, is adopted. At 90 MHz, the RF power transmission efficiency is 84 % with 60 mm distance between transmitting and receiving resonators. For the 90 MHz RF power, the rectifier efficiency for the RF to DC power conversion is 69 % and 76 % at 25 °C and −20 °C, respectively. For an energy storage unit, a supercapacitor is chosen for the low-temperature application. With the excellent temperature characteristic of the supercapacitor, the effectiveness of the supercapacitor is verified as the energy storage unit operating at −20 °C. It is shown that the WSN proposed in this work can operate in perpetuity as long as the circuit components in the WSN do not have any defects.

KEYWORDS:
Energy harvester, low temperature, supercapacitor, wireless sensor network (WSN)

1 | INTRODUCTION

Wireless sensor network (WSN) plays a key role in Internet of Things (IoT)[1]. It is most desirable that the WSN works autonomously without any interruption or downtime for battery replacement or being out of power. It has been pointed out that one of the unique challenges of IoT systems[2] is the energy constraint that would limit the service time of the IoT devices. To address this energy constraint for WSNs, energy harvesting techniques was surveyed[3]. Among the energy sources such as solar, wind, vibrations, or RF energy, the RF energy is considered as a reliable energy source because the RF energy can be generated and be controllable by human as opposed to the sources from nature.

When the resonant inductive coupling scheme was introduced by Kurs *et al*. in 2007[4], WPT in mid-range (0.5–5 m) is in great interest[5,6]. To make Kurs's work more feasible, Hu *et al*. developed a conformal strongly coupled magnetic resonant (CSCMR) technique[7].

The motivation of this work is a temperature and pressure monitoring system that is essential part in industrial freeze dryers[8]. It is crucial for the temperature and pressure monitoring system to operate autonomously in a freeze dryer without interruption. A conventional way to measure temperature inside the freeze dryer is using thermocouples. The drawbacks of using thermocouples[9] demand new techniques. Some WSNs in a freeze dryer[10,11] were powered by a lithium coin cell or alkaline battery. The low-temperature in a freeze dryer is much below 0 °C. In general, however, electrochemical batteries such as lithium-ion batteries or lithium coin cells have poor performance at low temperature[12,13,14].

In this work, we design and implement a self-sustainable WSN for low-temperature application. For the implementation

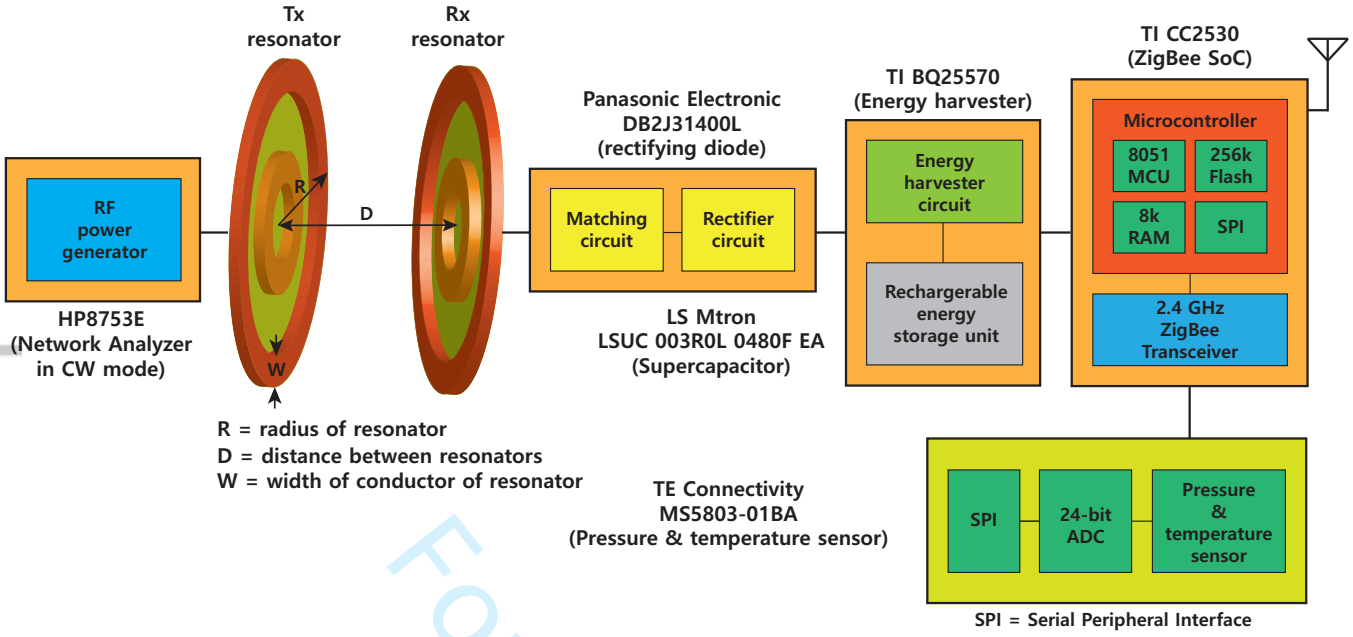

FIGURE 1 Block diagram of the wireless sensor node powered by the wireless power transfer technique with energy harvester.

of the whole WSN powered by WPT with an RF energy harvester and supercapacitor, the WPT is implemented with the CSCMR technique and the WSN adopts the Zigbee protocol. The charging and discharging characteristics of a supercapacitor in −20 °C and 25 °C are measured and analyzed to verify the effectiveness of the temperature performance of the supercapacitor. This WSN can operate autonomously in perpetuity even in a low temperature chamber.

2 | DESIGN CONSIDERATIONS FOR THE ENTIRE SYSTEM

The schematic of the wireless sensor node powered by a WPT technique with an RF energy harvester for low-temperature application is shown in Fig. 1 . For the design and implementation of the entire system, several design considerations are presented in the following subsections.

2.1 | Conformal Strongly Coupled Magnetic Resonator

As mentioned in Section 1, the WPT technique is realized by the CSCMR technique. Since the WSN proposed in this work needs to be working in a restricted area such as a freeze dryer, the resonators in the CSCMR technique must be small. To reduce the size of the transmitting and receiving resonators, the operating frequency is selected to be 90 MHz. Although the operating frequency of 90 MHz is in the middle of FM radio band, 88–108 MHz, it works only in the near field zone. Thus, its operation cannot interfere the operation of FM radio broadcasting.

To design the CSCMR scheme around 90 MHz, a commercial 3D electromagnetic simulator, HFSS[1] was used. Basically, the resonator is an LC resonator and its resonant frequency is governed by Equation (1).

$$f_r = \frac{1}{2\pi\sqrt{LC}} \tag{1}$$

The capacitance is chosen to be 33 pF. By using the Eigenmode solver in HFSS, the dimensions of the source loop and resonator were determined to be operating around 90 MHz. The radii of the source and resonator are 16 mm and 28 mm, respectively. The width of the conductor for the source and resonator is the same as 6 mm. The source (or load) loop and transmitting (or receiving) resonator are on each side of a 1.5 mm thick FR4 ($\epsilon_r = 4.5$ and $\tan\delta = 0.01$) substrate with 35 μm thick of copper.

With the dimensions of the resonator, the 3D model of the CSCMR technique, as shown in Fig. 1 , is simulated in HFSS. The optimum distance between the transmitting and receiving resonators is determined for the most efficient transmission performance. From the simulated and measured S-parameters, the efficiency (η_{WPT}) of the CSCMR technique for the RF power transmission can be calculated by the Equation (2)[7]. The results will be shown in Section 3.

[1]High Frequency Structure Simulator, ANSYS, Inc., 2016.

$$\eta_{WPT} = \frac{P_{load}}{P_{source}} = |S_{21}|^2 \quad (2)$$

2.2 | Circuit Design of RF Power Rectifier and Energy Harvester

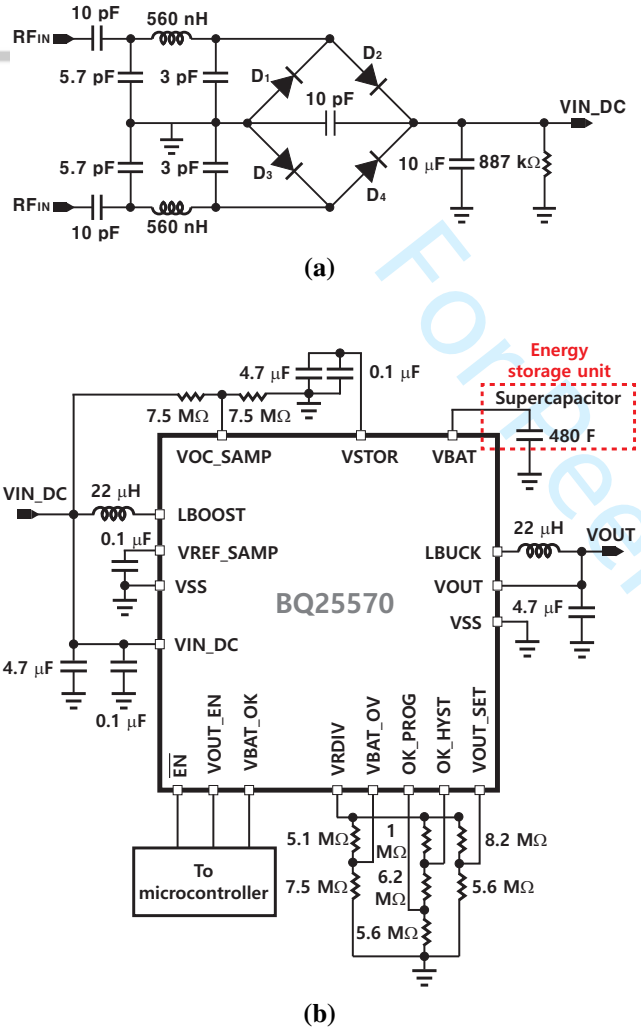

FIGURE 2 Schematics of the (a) rectifier and (b) energy harvester with an energy storage unit, a supercapacitor in this work.

The schematics of the rectifier and energy harvester are shown in Fig. 2 (a) and (b), respectively. The rectifier is realized using the conventional bridge rectifier circuit with 4 Schottky diodes. The rectifier efficiency (η_{RF-DC}) for the RF to DC power conversion can be calculated using Equation (3)[15].

$$\eta_{RF-DC} = \frac{I_{out}^2 R_L}{(\frac{v_{peak}}{\sqrt{2}R_s})^2} \times 100 \quad (3)$$

In Equation (3), v_{peak}, R_s, I_{out}, and R_L are the peak input voltage, the output resistance of 50 Ω of an RF power generator, the output current from the rectifier, and load resistance of 887 kΩ, as shown in Fig. 2 (a), respectively. Because the input resistance of the energy harvester, , BQ25570 manufactured by Texas Instruments (TI), is 20 Ω, the load resistance of the rectifier must be very high. Thus, the load resistance of 887 kΩ is chosen in this work.

Since the current extracted from the rectifier turns out to be quite small, the rectifier itself cannot supply enough to power for a single wireless sensor node. Therefore, the rectifier is followed by the energy harvester with a rechargeable energy storage unit as shown in Fig. 2 (b). The the BQ25570 is capable of extracting μW to mW of power from high output impedance DC sources to charge electrochemical batteries or supercapacitors. As the WSN proposed in this work is for low-temperature application, a supercapacitor is chosen.

2.3 | Wireless Sensor Network

Among wireless communication protocols such as Zigbee, Wi-Fi, or Bluetooth, Zigbee is adopted to implement the WSN. Zigbee is an excellent solution for WSN, as it enables to realize a stand-alone mesh network with low cost and low power consumption. The Zigbee SoC and digital multi-sensor are manufactured by TI and TE Connectivity, respectively. The digital multi-sensor can measure pressure and temperature. The pressure and temperature ranges are from 10 to 1300 mbar and from −40 °C to 85 °C, respectively.

Two separate software modules for a transmitter and receiver were implemented. The transmitter and the receiver were implemented in the Application layer on top of TI's layered software architecture[16]. The Basic RF is a protocol layer to transmit and receive data packets through a two-way RF link. In the transmitter, a serial peripheral interface (SPI), as shown in Fig. 1 , was implemented with the hardware abstraction layer to communicate with the sensor modules. The transmitter's main control module, an SPI master, sends the analog/digital conversion command to the sensor module when it needs sensor readings. Then, the sensor module, an SPI slave, sends back the current sensor readings to the master.

In the receiver, an interrupt service routine (ISR) in the Basic RF is responsible for getting data from the transmitter. When a complete packet is successfully received through the ISR, the Basic RF sets a ready flag. The receiver module in the Application layer can notice that an RF packet is ready by checking the flag in a loop. When the flag is set, the receiver

module will read the transmitted data. More details for the packet transmission and reception sequences can be found in TI's document[16].

3 | RESULTS AND DISCUSSIONS

3.1 | Conformal Strongly Coupled Magnetic Resonator

The performance of the CSCMR technique is measured by HP8753E vector network analyzer. The comparison of the S-parameters between simulated and measured results is shown in Fig. 3 . As can be seen, the S-parameters simulated with 33 pF is off to the right compared to the measured S-parameters. The reason for this is because the commercial chip capacitor has some manufacturing tolerance in the capacitance. When simulated with a capacitance of 34.5 pF, as shown in Fig. 3 , the simulated S-parameters is matched very well to the measured S-parameters. The measured insertion loss ($|S_{21}|$) between the transmitting and receiving resonators with 60 mm distance is 1.49 dB, which results in the η_{WPT} of the CSCMR technique to be 84 % calculated by using Equation (2) in Section 2.1.

In Table 1 , several magnetic resonant coupling techniques available in the literature are compared with this work. As can be seen in Table 1 , WPT distance is correlated with the radii of the Tx & Rx coils. Longer WPT distance requires larger radii of the Tx & Rx coils. Since the WSN proposed in this work operates in a small chamber, the miniaturization of the Tx & Rx coils is essential. While the radii of the Tx & Rx coils proposed in this study are the smallest ones in Table 1 , the WPT distance and efficiency of this work are superior or comparable to other techniques with respect to $\frac{\text{Distance}}{\text{Radius of coil}}$ ratio.

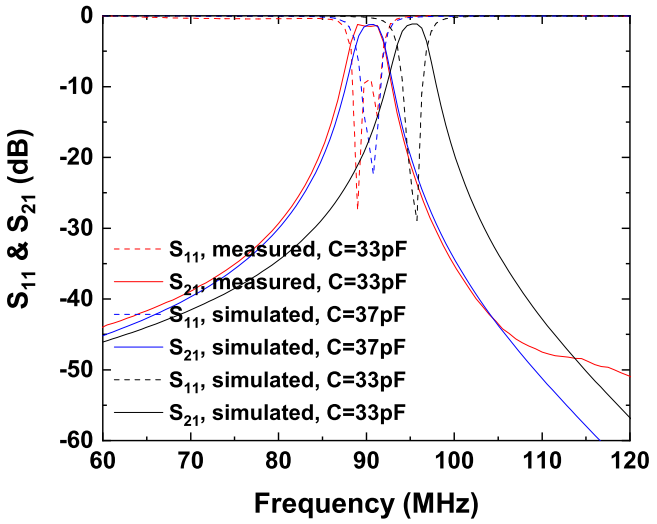

FIGURE 3 Comparison of S-parameters between simulated and measured results of the CSCMR system.

3.2 | Rectifier and Energy Harvester

The photographs of fabricated PCBs for the rectifier and the transmitter of the WSN with the energy harvester are shown in Fig. 6 (a). The RF power waveform at the rectifier input and the waveform at the output of the rectifier are compared to each other in Fig. 4 (a). Fig. 4 (b) shows the output voltages and currents of the rectifier with respect to the peak input voltage from 3.6 to 10.2 V at 90 MHz. It also shows the temperature

TABLE 1 Comparison of different magnetic resonant coupling techniques

Shape of coil	Radii of coils	Frequency (MHz)	Distance (mm)	Efficiency (%)	Applications
Single-turn wire (No thickness given)	Tx & Rx 150 mm	13.56	180	80	No application presented[17]
Circular spiral coil (No thickness given)	Tx 6 × 126 mm Rx 29 mm	1	50	74	Charging a smart phone[18]
Square spiral coil (Thickness = 0.54 mm)	Tx & Rx 50 mm × 50 mm	13.8	10	79	Monitoring system for implanted device[19]
Twelve-layer PCB (Thickness = 2 mm)	Tx & Rx 32 mm	20	60	78.2	No application presented[20]
Three-turn wire (No thickness given)	Tx & Rx 100 mm	7.0	200	86.8	No application presented[21]
Two-layer PCB (Thickness = 1.5 mm)	Tx & Rx 28 mm	90	60	84	WSN for low-temperature application [This work]

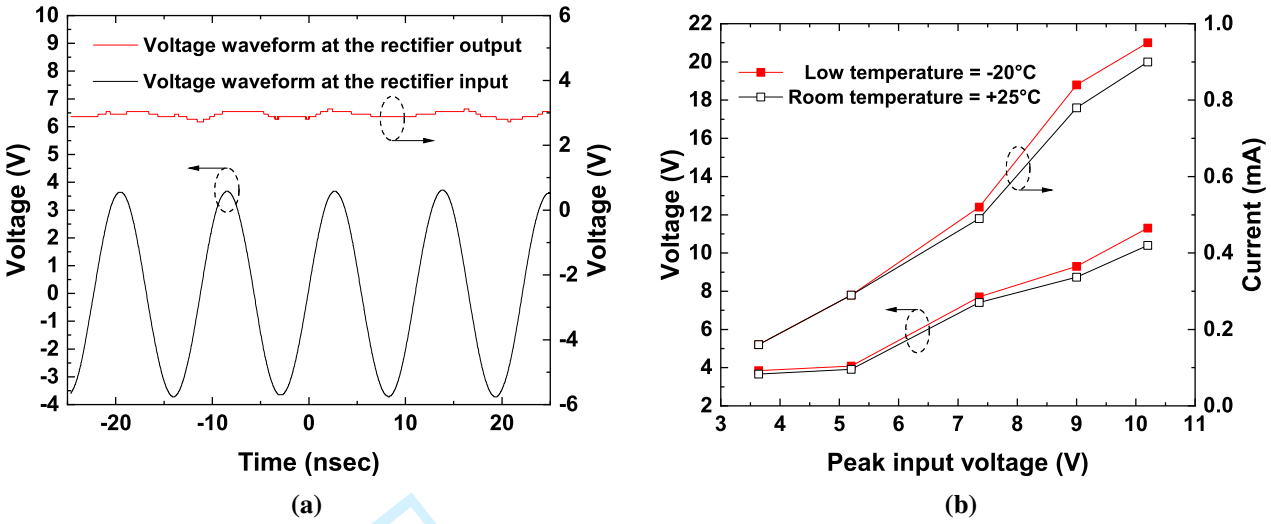

FIGURE 4 (a) Voltage waveforms at the input and output of the rectifier and (b) output voltages and currents of the rectifier with respect to the input voltage level.

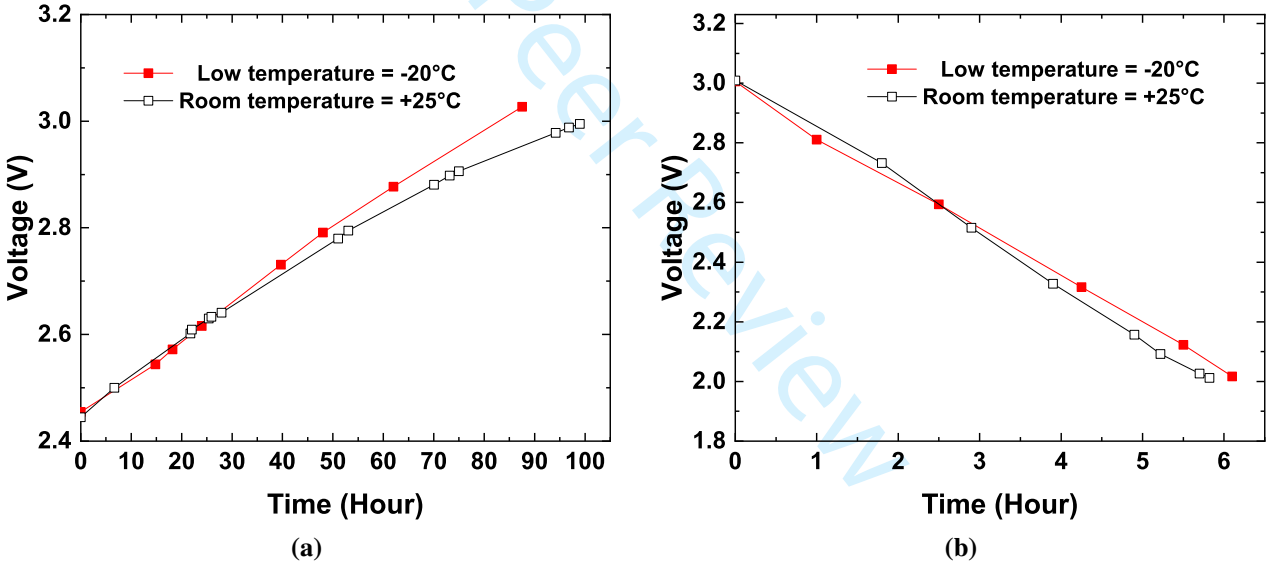

FIGURE 5 Temperature (−20 °C vs. 25 °C) characteristics of (a) charging and (b) discharging the supercapacitor.

(−20 °C vs. 25 °C) characteristics. As can be seen in Fig. 4 (b), the output voltage and current of the rectifier is slightly increased at −20 °C. The peak input voltage of 10.2 V to the rectifier is used to operate the rectifier and energy harvester. The current supplied to the energy harvester from the rectifier at 20 °C is 0.9 mA as shown in Fig. 4 (b). By the Equation (3) with the v_{peak} of 10.2 V and I_{out} of 0.9 mA, the η_{RF-DC} is 69 % at 20 °C. With the I_{out} of 0.95 mA at −20 °C, η_{RF-DC} is 76 %.

Fig. 5 (a) and (b) show the temperature characteristics of charging and discharging the supercapacitor. As can be seen in Fig. 5 , the temperature characteristics of the supercapacitor is excellent for low-temperature applications. The charging characteristic, as shown in Fig. 5 (a), at −20 °C is similar to that at 25 °C. Although the charging time is very long, it is only 8 % longer when compared to theoretical value of 80.3 hours. The time duration ($\Delta t = t - t_0$) for the charging process can be calcuated by using Equation (4), where the C, I_{charge}, and $v(t_0)$ are 480 F, 0.95 mA, and 2.455 V, respectively. The charging time at 25 °C is 11.5 hours longer than that at −20 °C.

This might come from heating the supercapacitor during the charging process.

$$\Delta t = \frac{C(v(t) - v(t_0))}{I_{charge}} = \frac{C\Delta v}{I_{charge}} \quad (4)$$

The discharging characteristic, as shown in Fig. 5 (b), is very linear even at −20 °C. The supercapacitor was discharged by operating continuously the transmitter of the WSN shown in Fig. 6 . When the transmitter operating, the transmitter consumes around 24 mA, which is $I_{discharge}$ in Equation (5). The measured voltage drop of 0.997 V is also very close to the theoretical value of 1.04 V calculated by Equation (5), where the C, $I_{discharge}$, and Δt are 480 F, 24 mA, and 5.82 hours, respectively.

$$\Delta v = \frac{I_{discharge}(t - t_0)}{C} = \frac{I_{discharge}\Delta t}{C} \quad (5)$$

Fig. 5 (b) shows that low-temperature does not affect too much the discharge performance of the supercapacitor. The temperature independent performance of the supercapacitor makes supercapacitors perfect solution for energy storage unit for low temperature applications.

3.3 | Wireless Sensor Network

The WSN powered by WPT for low-temperature application is implemented as shown in Fig. 6 . The transmitter of the WSN is set up in a chamber to collect and send information of temperature and pressure in the chamber, as shown in Fig. 6 (a). The receiver of the WSN, as shown in Fig. 6 (b), is located outside the chamber.

Based on the charging and discharging characteristics presented in Section 3.2, one may establish an operating scenario for the WSN as follows. The packet sent from the transmitter has 24 bytes. The data rate of the WSN is set to be 250 kbps in this work. Therefore, it takes 0.758 msec. to send the packet from the transmitter to receiver. The transmitter consumes maximum 2.6 μA in its sleep mode and takes 0.6 msec. to transit from sleep mode to transmitting mode[22].

Let us assume that the transmitter is in transmitting mode for 2 msec. including sending a packet and transition from transmitting to sleep mode and it transmits environmental parameters 60 times per one hour to the receiver. Then, it consumes 2.9 mA per an hour in the transmitting mode and in the rest of an hour, it consumes 9.4 mA in the sleep mode. For a day, the voltage drops 0.62 mV due to the operation of the WSN in this operating scenario. It takes only 331 sec. to charge the supercapacitor of 480 F with the charging current of 0.9 mA for the voltage drop of 0.62 mV. The supercapacitor can be charged 7 times for 50 sec. during each sleep mode at the end of the day. As long as the circuit parts of the WSN operate properly, this WSN powered by WPT technique can operate without battery exchange process.

4 | CONCLUSION

We have demonstrated a self-sustainable WSN for low-temperature application. The WPT efficiency was 84 % with the distance of 60 mm between transmitting and receiving resonators. The power conversion efficiency of the RF power rectifier is 69 % and 76 % at 25 °C and −20 °C, respectively. To the rectifier, an energy harvester is added with a supercapacitor as an energy storage unit. The supercapacitor showed an excellent linearity in charging and discharging characteristics even at −20 °C.

In an operating scenario, it was shown that the WSN can operate without battery exchange process. In this scenario, the WSN can collect environmental parameters such as temperature and pressure in a low temperature chamber every 1 min. in a day. This design can be an excellent application of IoT used for monitoring the environment of a chamber where the pressure and temperature should be delicately controlled such as freeze dryers in pharmaceutical manufacturing industry.

ACKNOWLEDGMENT

This article was supported by Wonkwang University in 2020.

References

[1] Lin J, Yu W, Zhang N, Yang X, Zhang H, Zhao W. A Survey on Internet of Things: Architecture, Enabling Technologies, Security and Privacy, and Applications. *IEEE Internet of Things Journal* 2017; 4(5): 1125-1142. doi: 10.1109/JIOT.2017.2683200

[2] Bagchi S, Abdelzaher TF, Govindan R, et al. New Frontiers in IoT: Networking, Systems, Reliability, and Security Challenges. *IEEE Internet of Things Journal* 2020; 7(12): 11330-11346. doi: 10.1109/JIOT.2020.3007690

[3] Sudevalayam S, Kulkarni P. Energy Harvesting Sensor Nodes: Survey and Implications. *IEEE Communications Surveys & Tutorials* 2011; 13(3): 443-461. doi: 10.1109/SURV.2011.060710.00094

[4] Kurs A, Karalis A, Moffatt R, Joannopoulos JD, Fisher P, Soljačić M. Wireless Power Transfer via Strongly Coupled Magnetic Resonances. *Science* 2007; 317(5834): 83–86. doi: 10.1126/science.1143254

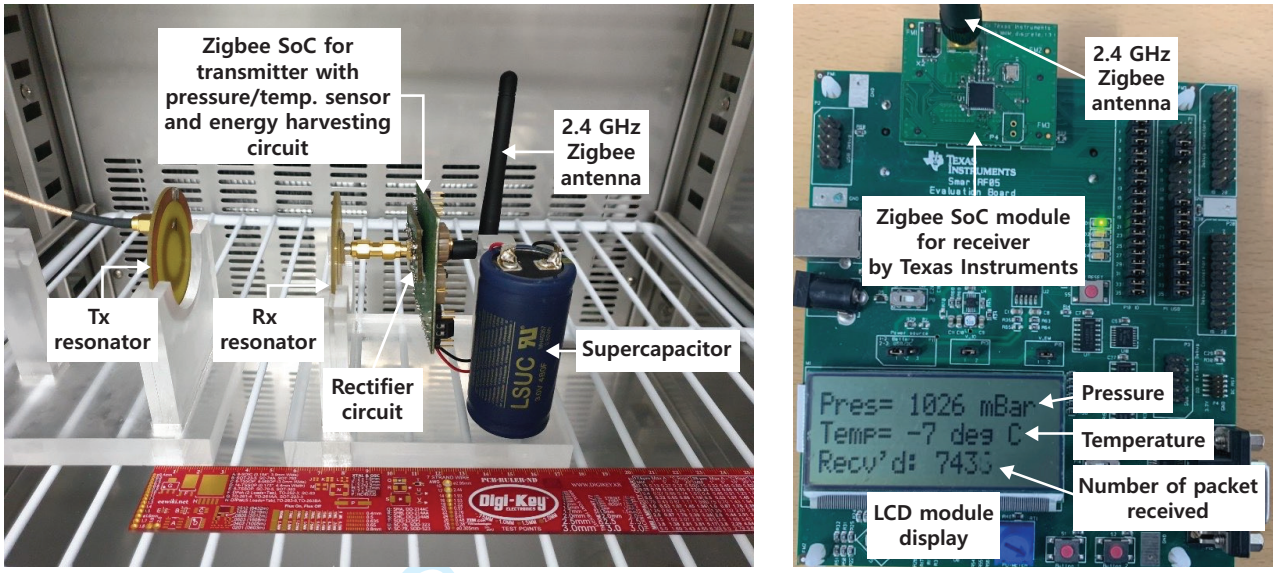

FIGURE 6 Photographs of the (a) transmitter powered by wireless power transfer system and (b) receiver of the wireless sensor network.

[5] Hui SYR, Zhong W, Lee CK. A Critical Review of Recent Progress in Mid-Range Wireless Power Transfer. *IEEE Transactions on Power Electronics* 2014; 29(9): 4500-4511. doi: 10.1109/TPEL.2013.2249670

[6] Shadid R, Noghanian S, Nejadpak A. A literature survey of wireless power transfer. *2016 IEEE International Conference on Electro Information Technology (EIT)* 2016: 0782-0787. doi: 10.1109/EIT.2016.7535339

[7] Hu H, Bao K, Gibson J, Georgakopoulos SV. Printable and Conformal Strongly Coupled Magnetic Resonant systems for wireless powering. *2014 IEEE Annual Conference on Wireless and Microwave Technology (WAMICON)* 2014: 1-4. doi: 10.1109/WAMICON.2014.6857762

[8] Fissore D, Pisano R, Barresi AA. On the use of temperature measurement to monitor a freeze-drying process for pharmaceuticals. *2017 IEEE International Instrumentation and Measurement Technology Conference (I2MTC)* 2017: 1-6. doi: 10.1109/I2MTC.2017.7969890

[9] Grassini S, Fulginiti D, Pisano R, Oddone I, Parvis M. Real-time temperature monitoring in pharmaceutical freeze-drying. *2014 IEEE International Symposium on Medical Measurements and Applications (MeMeA)* 2014: 1-5. doi: 10.1109/MeMeA.2014.6860051

[10] Corbellini S, Parvis M, Vallan A. In-Process Temperature Mapping System for Industrial Freeze Dryers. *IEEE Transactions on Instrumentation and Measurement* 2010; 59(5): 1134-1140. doi: 10.1109/TIM.2010.2040909

[11] Cho YS, Kwon J, Choi S. Design and Implementation of Wireless Sensor Network for Freeze Dryer. *Journal of Information and Communication Convergence Engineering* 2015; 13(1): 21-26.

[12] Ein-Eli Y, Thomas SR, Chadha R, Blakley TJ, Koch VR. Li-Ion Battery Electrolyte Formulated for Low-Temperature Applications. *Journal of The Electrochemical Society* 1997; 144(3): 823–829. doi: 10.1149/1.1837495

[13] Smart MC, Ratnakumar BV, Surampudi S. Electrolytes for Low-Temperature Lithium Batteries Based on Ternary Mixtures of Aliphatic Carbonates. *Journal of The Electrochemical Society* 1999; 146(2): 486–492. doi: 10.1149/1.1391633

[14] Huang CK, Sakamoto JS, Wolfenstine J, Surampudi S. The Limits of Low-Temperature Performance of Li-Ion Cells. *Journal of The Electrochemical Society* 2000; 147(8): 2893. doi: 10.1149/1.1393622

[15] Palazzi V, Del Prete M, Fantuzzi M. Scavenging for Energy: A Rectenna Design for Wireless Energy Harvesting in UHF Mobile Telephony Bands. *IEEE Microwave Magazine* 2017; 18(1): 91-99. doi: 10.1109/MMM.2016.2616189

[16] Texas Instruments Incoporated . CC2530 Software Examples User's Guide. 2009.

[17] Imura T, Hori Y. Maximizing Air Gap and Efficiency of Magnetic Resonant Coupling for Wireless Power Transfer Using Equivalent Circuit and Neumann Formula. *IEEE Transactions on Industrial Electronics* 2011; 58(10): 4746-4752. doi: 10.1109/TIE.2011.2112317

[18] Jadidian J, Katabi D. Magnetic MIMO: How To Charge Your Phone in Your Pocket. In: ACM; 2014

[19] Xu G, Yang X, Yang Q, Zhao J, Li Y. Design on Magnetic Coupling Resonance Wireless Energy Transmission and Monitoring System for Implanted Devices. *IEEE Transactions on Applied Superconductivity* 2016; 26(4): 1-4. doi: 10.1109/TASC.2016.2524591

[20] Bao K, Zekios CL, Georgakopoulos SV. Miniaturization of SCMR Systems Using Multilayer Resonators. *IEEE Access* 2019; 7: 143445-143453. doi: 10.1109/ACCESS.2019.2945319

[21] Shi L, Rasool N, Zhu H, Huang K, Yang Y. Design and Experiment of a Reconfigurable Magnetic Resonance Coupling Wireless Power Transmission System. *IEEE Microwave and Wireless Components Letters* 2020; 30(7): 705-708. doi: 10.1109/LMWC.2020.2997068

[22] Texas Instruments Incoporated . CC2530 datasheet (Rev. B). 2011.

How to cite this article: Y. S. Cho, K. Choi, and J. Kwon (2021), Self-sustainable wireless sensor network for low-temperature application, *Microw Opt Technol Lett.*, *2021;00:1–6*.

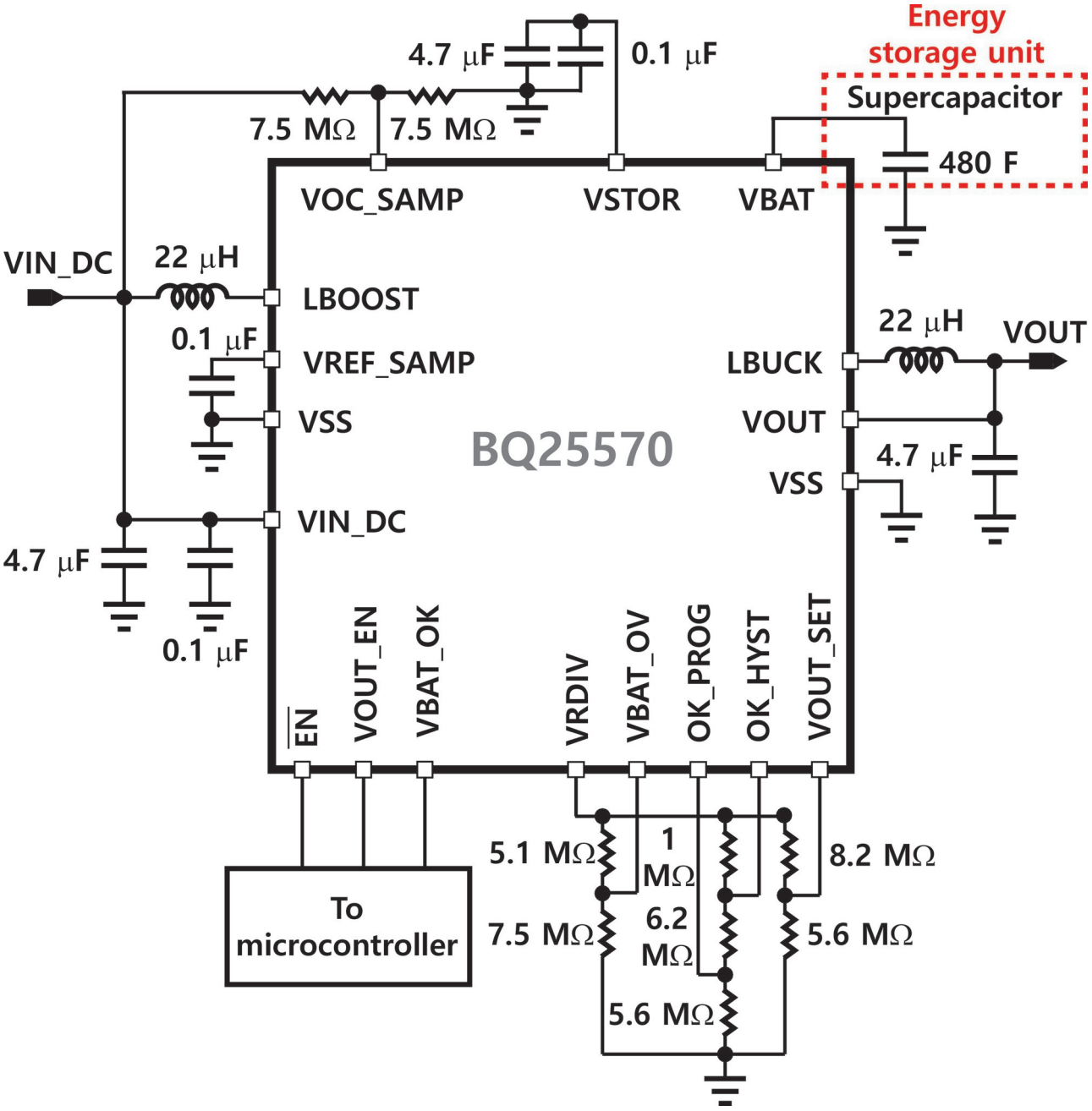

mop_33114_circuit_diagram_energy_harvester.eps

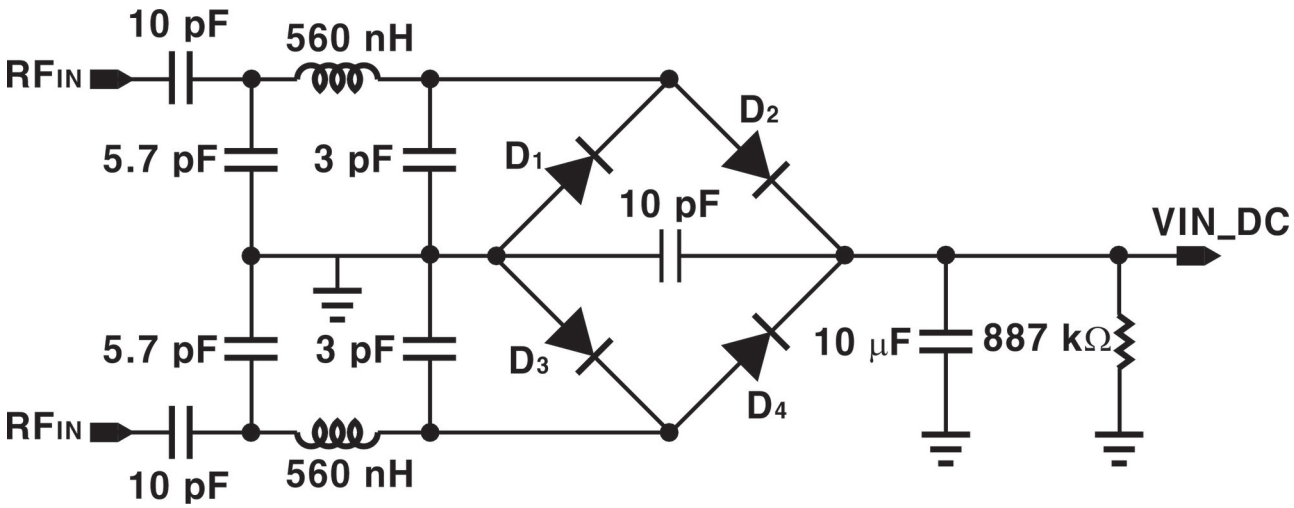

mop_33114_circuit_diagram_rectifier.eps

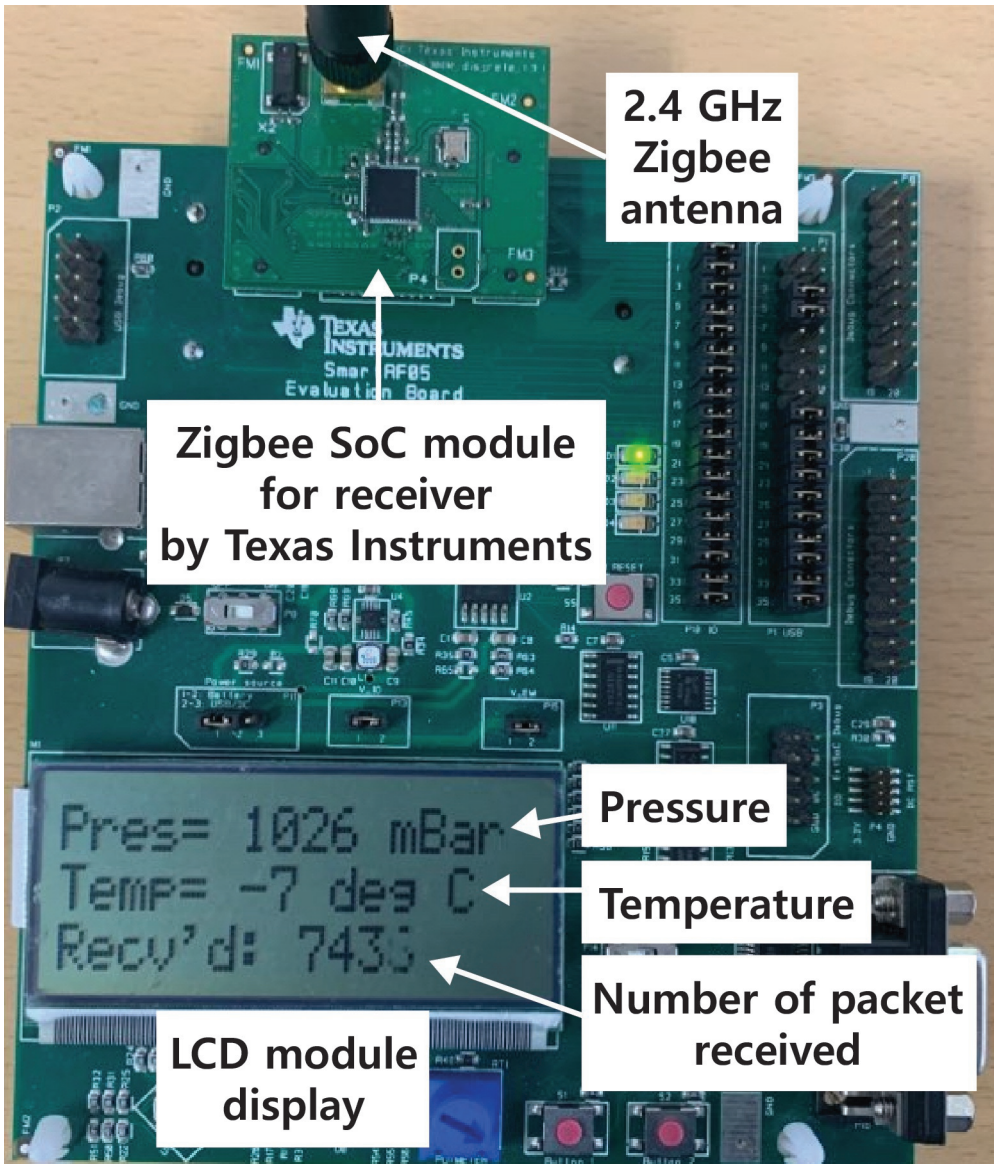

mop_33114_pcb_zigbee_receiver.eps

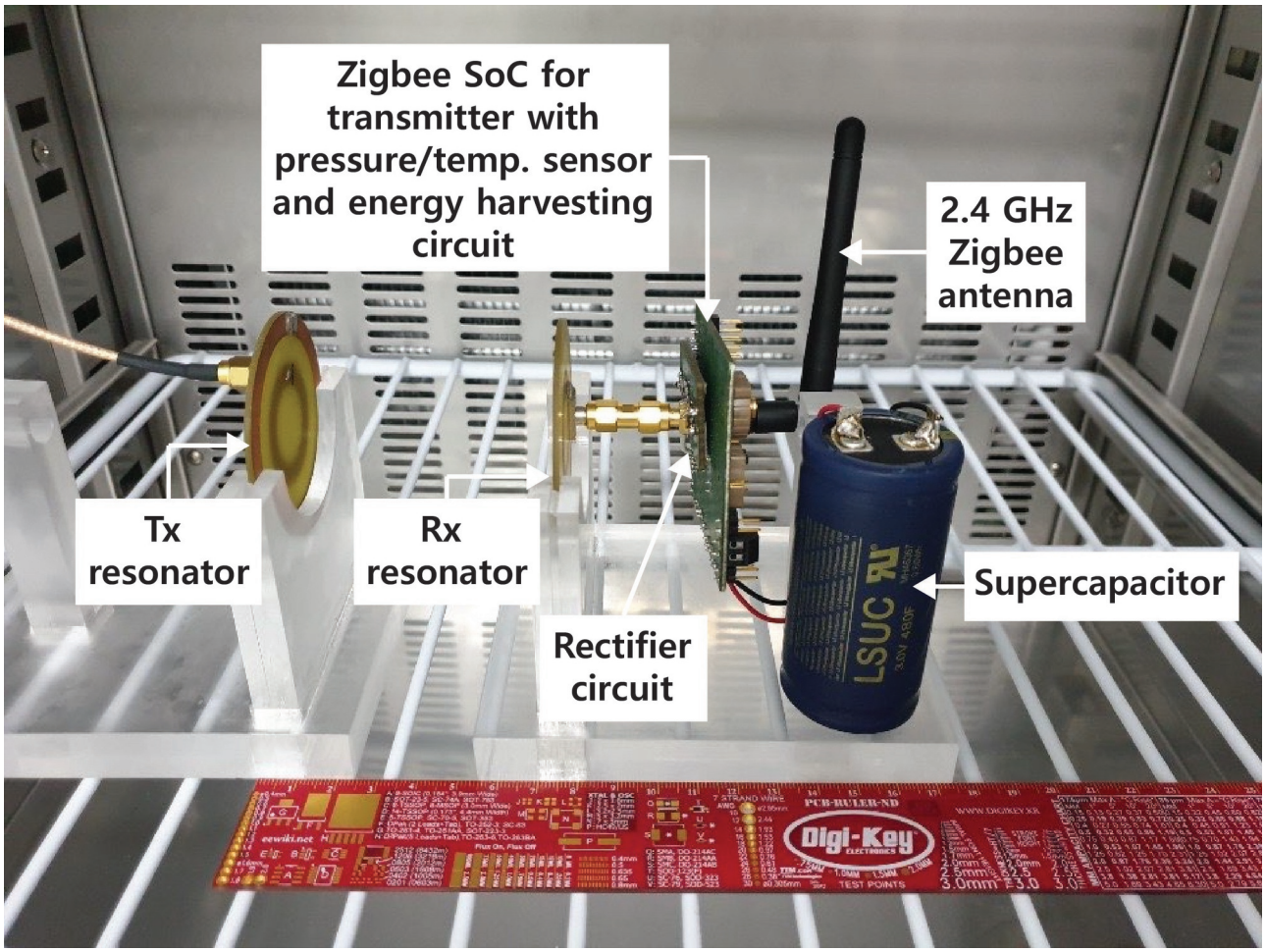

mop_33114_photograph_entire_system_in_chamber.eps

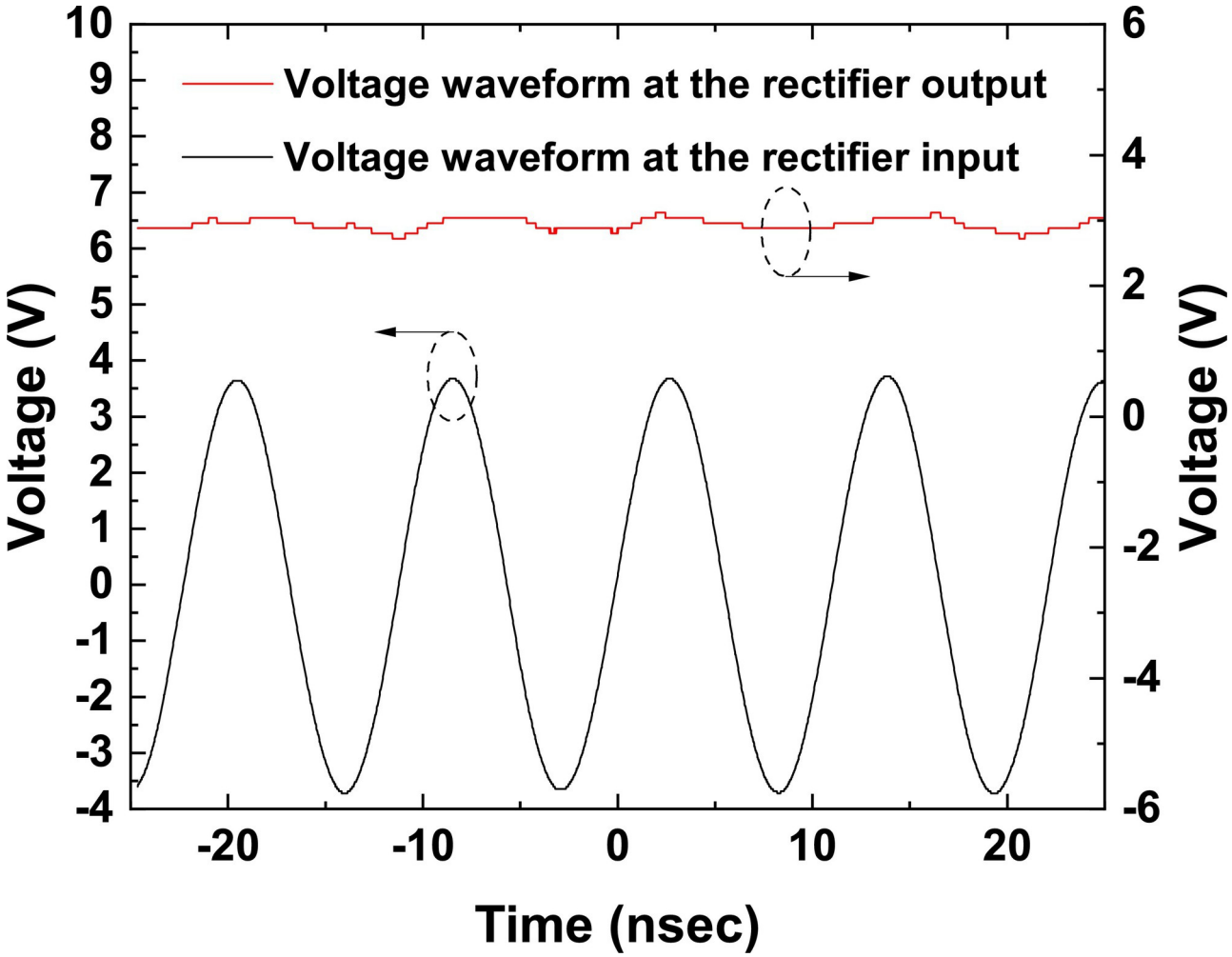

mop_33114_rectifier_input_output_waveforms.eps

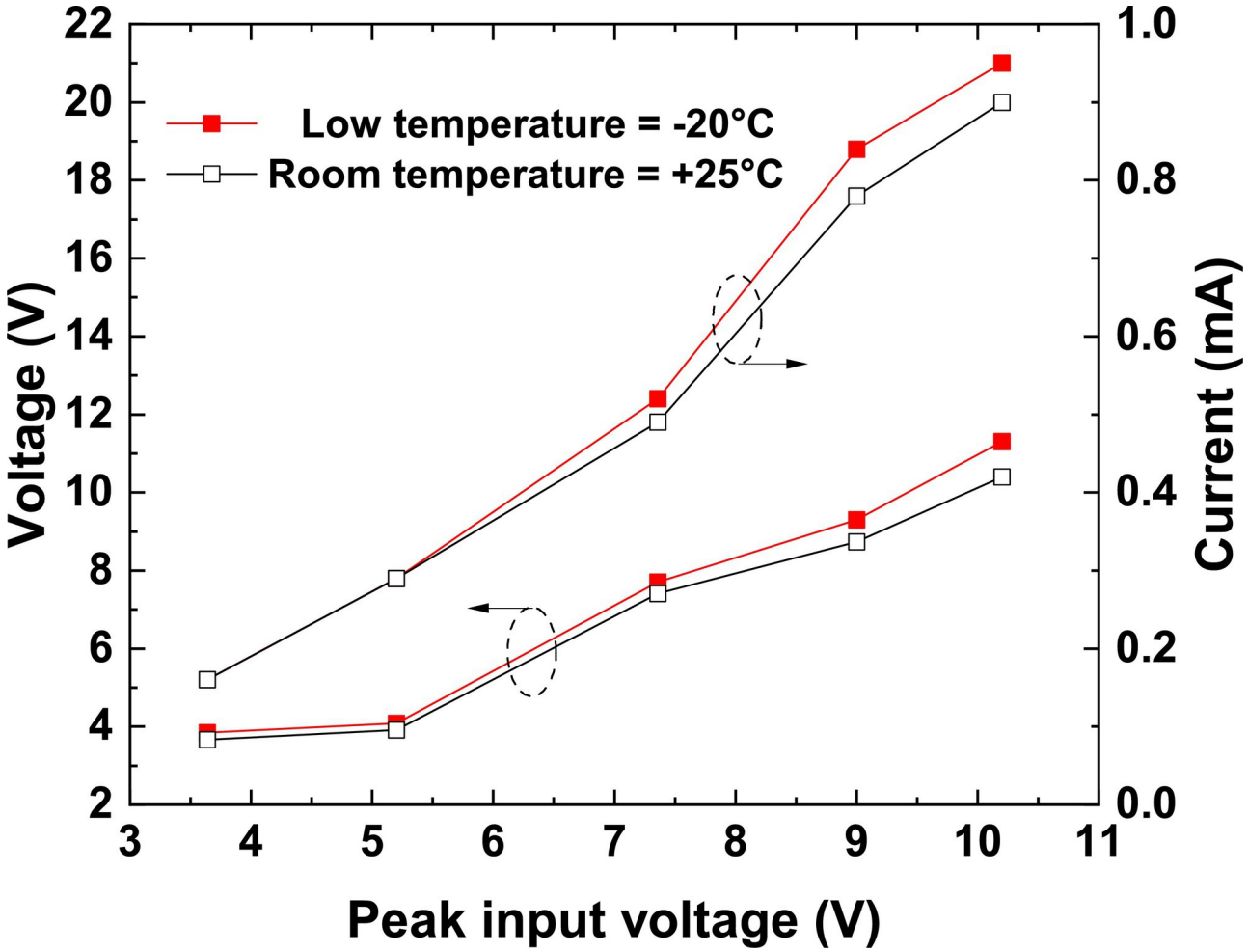

mop_33114_rectifier_output_voltage_vs_input_voltage.eps

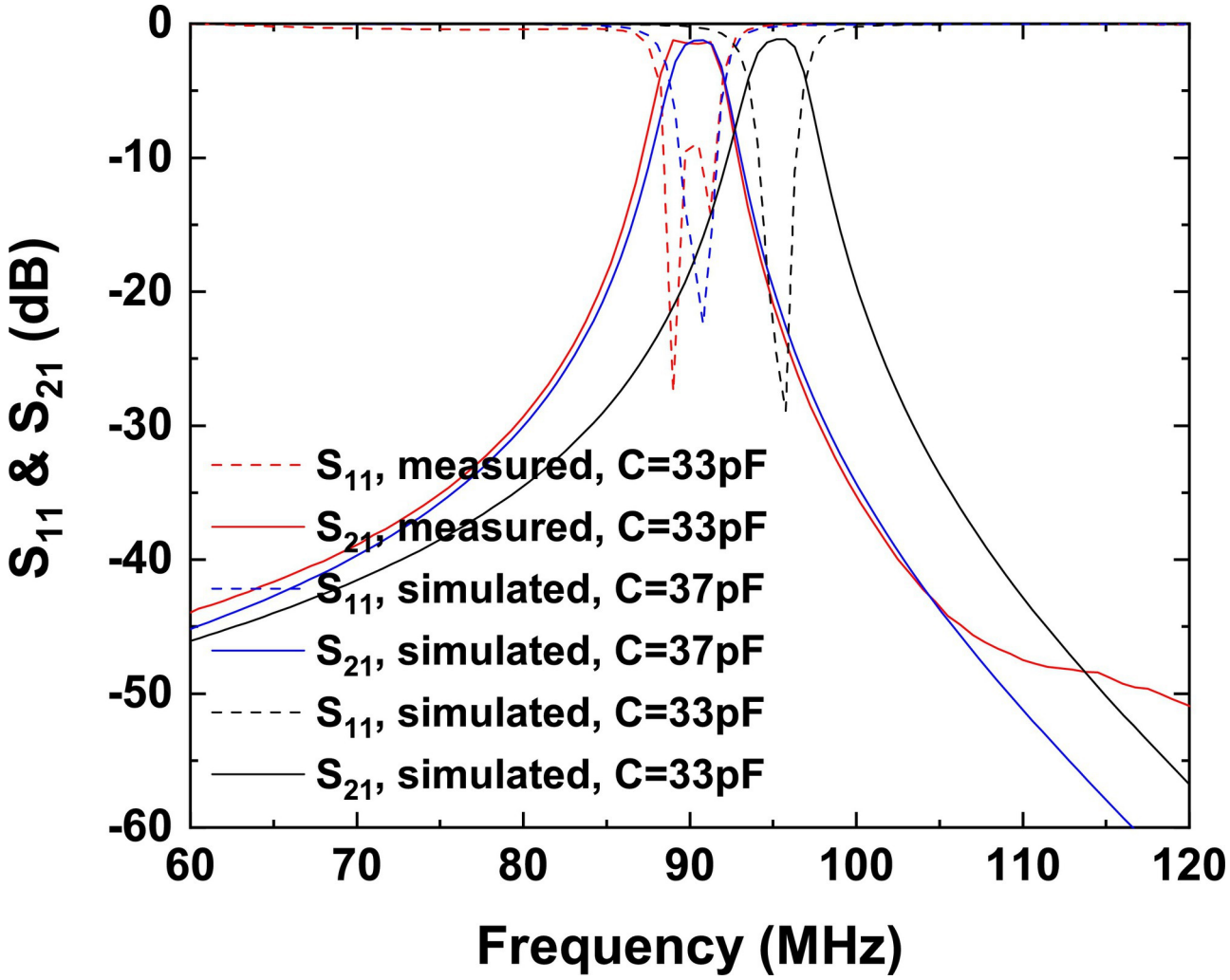

mop_33114_s_parameters_cscmr_measured_simulated.eps

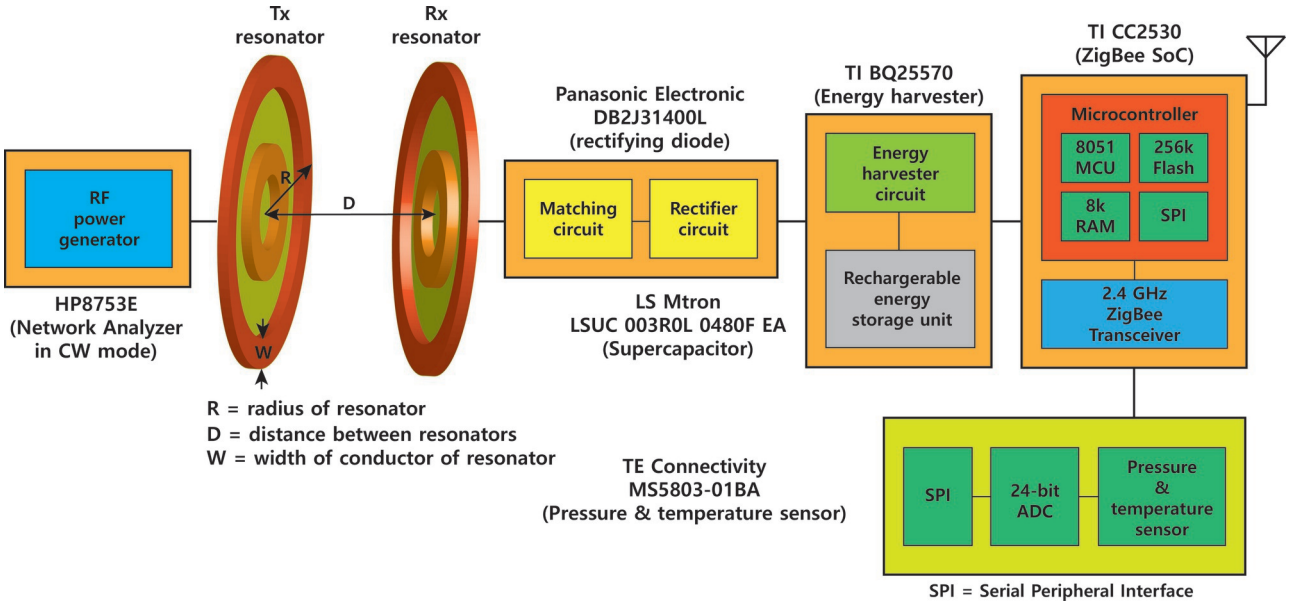

mop_33114_schematic_wireless_sensor_node_powered_by_wpt.eps

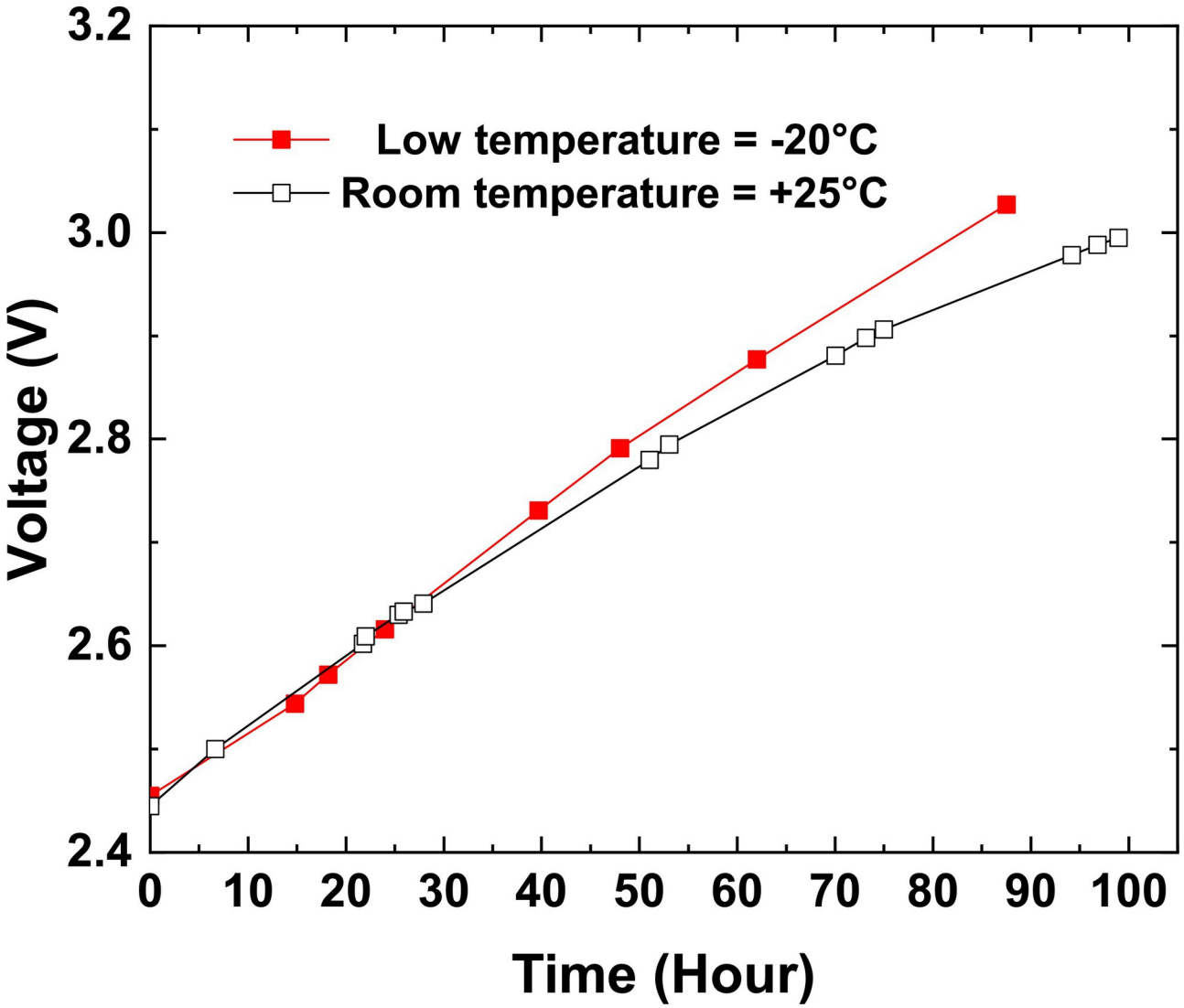

mop_33114_supercap_charge_characteristic.eps

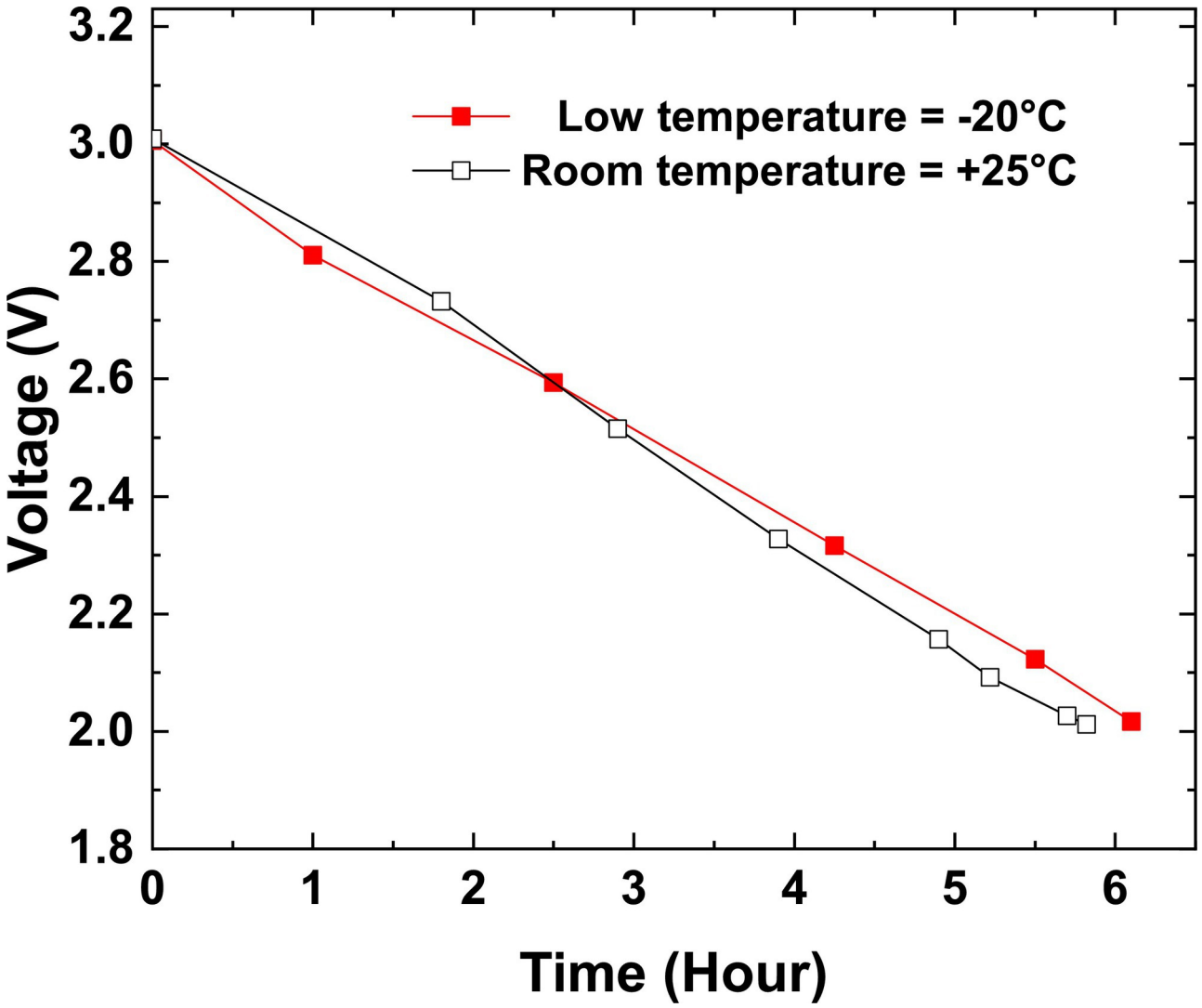

mop_33114_supercap_discharge_characteristic.eps